Quality Classification of Harumanis Mango Based on External Multi-Parameter and Machine Learning Techniques

Mohd Nazri Abu Bakar^{1*}, Abu Hassan Abdullah², Muhamad Imran Ahmad^{3*}, Norasmadi Abdul Rahim⁴, Haniza Yazid⁵, Wan Mohd Faizal Wan Nik⁶, Shafie Omar⁷, Shahrul Fazly Man@Sulaiman⁸, Tan Shie Chow⁹, Fahmy Rinanda Saputri¹⁰ Institute of Sustainable Agrotechnology, Universiti Malaysia Perlis, Malaysia ^{1, 3, 6, 7, 8} Faculty of Electrical Engineering and Technology, Universiti Malaysia Perlis, Malaysia^{2, 4} Faculty of Intelligent Computing, Universiti Malaysia Perlis, Malaysia³ Faculty of Electronic Engineering and Technology, Universiti Malaysia Perlis, Malaysia^{5, 9} Faculty of Engineering and Informatics, Universitas Multimedia Nusantara, Indonesia¹⁰

Abstract—Grading Harumanis mangoes is traditionally done through manual visual inspection, which is subjective, inconsistent, and labor-intensive. Industry practices report only 70-80% consistency among human graders, with accuracy further declining under fatigue or high volumes. These limitations hinder uniform quality assurance, especially for export markets. To address this, an image-based, non-destructive grading system was developed, focusing on external features such as surface defect severity, ripeness index, shape uniformity, and size. A dataset of 1,018 mango samples was collected and analyzed using a machine vision system. Features were extracted through image segmentation and color-shape analysis, then classified using a Fuzzy Inference System (FIS) and Machine Learning (ML) models including SVM, MLPNN, and ANFIS. Enhanced SVM variants were also implemented to assess performance gains. Results showed strong performance across all parameters: ripeness index accuracy reached 93.5%, shape uniformity 91.6%, and size classification over 96%. The enhanced SVM+ achieved the best overall accuracy at 95.1% with the lowest error rates. The proposed system demonstrated clear improvements over manual grading and effectively classified mangoes into PREMIUM, GRADE 1, GRADE 2, and REJECT categories, supporting its potential for reliable real-world deployment.

Keywords—Machine learning; image processing; quality assessment; Harumanis mango; appearance attributes

I. Introduction

Mango is a widely cultivated tropical fruit that is highly valued for its unique flavor, aroma, and nutritional benefits. Among the various cultivars, the Harumanis mango is particularly renowned for its exceptional quality and popularity in Malaysia [1]. Harumanis mangoes are in high demand for both export and local consumption, and must therefore meet predetermined quality standards. Failure to meet these standards can result in substantial economic losses and reduced returns for vendors. Consequently, it is necessary to sort mangoes based on key grading parameters, including size, shape, maturity, defects, firmness, and nutritional content. The post-harvest grading process classifies mangoes into predefined quality categories, where effective grading enhances vendor and farmer confidence

while expanding export opportunities. However, the traditional manual grading process is frequently subjective, laborious, and inconsistent, with reported grader consistency as low as 70–80% [2-3].

To overcome these challenges, researchers have increasingly explored advanced computer vision and ML techniques for automated mango quality assessment [4-6].[22]. While these studies demonstrated promising results, most were limited to individual features (e.g., color or size) or lacked extensive validation, reducing their robustness for real-world deployment.

Building on this foundation, the present study makes three key contributions. First, it proposes a multi-feature image-based grading framework for Harumanis mangoes that integrates surface defect severity, ripeness index, shape uniformity, and size—parameters rarely evaluated together in previous works. Second, the study evaluates multiple classification models, including FIS, SVM, MLPNN, and ANFIS, with enhanced SVM variants achieving an accuracy of 95.1%, outperforming earlier studies that typically reported accuracies below 90%. Third, to ensure robustness and reduce risks of overfitting, the study employs a k-fold cross-validation strategy with independent testing, while also acknowledging limitations such as lighting variability, dataset imbalance, and cultivar generalizability.

By addressing both methodological gaps and performance limitations in existing approaches, this study provides a more reliable, scalable, and high-accuracy grading system that offers clear improvements over traditional manual inspection and prior automated methods.

II. RELATED WORKS

Recent studies span defect synthesis, ripeness, shape, and size assessment. For surface defects, image-to-image translation with conditional GANs can augment rare defect cases [7], but synthetic artifacts risk domain shift and inflated accuracy if not validated on truly independent, real-world images. CNN-based defect classifiers [8-9] often report high accuracy on single-cultivar, lab-lighting datasets, with limited discussion of class

^{*}Corresponding authors.

imbalance, inter-rater agreement for labels, or external test sites [21]. Classical pipelines using color/texture + SVM/kNN [10]. The study in [13] are interpretable but may be sensitive to illumination and background variability; they also evaluate a narrow set of varieties and typically do not integrate multiple attributes into a single grading decision.

For ripeness, hyperspectral + deep models [8] achieve fine spectral discrimination, yet sensor cost, throughput, and calibration burden constrain deployment; generalization across orchards and seasons is seldom shown. RGB image approaches [11-12] are cheaper but frequently rely on controlled setups and lack cross-cultivar validation. Shape-based grading [14-15] demonstrates that geometry helps detect deformities and even distinguish varieties. However, many methods assume clean silhouettes; occlusions, stem/calyx variability, and pose changes can degrade performance. Fourier descriptors [16] are transformation-invariant but may miss localized defects and can be sensitive to imperfect segmentation.

Size estimation [17-19] via dimension/mass prediction is useful, yet several works depend on explicit calibration objects, single-view assumptions, or manual placement, limiting throughput and robustness on conveyors. Across these threads, common gaps persist: (i) single-attribute focus rather than multi-attribute fusion aligned to market grades; (ii) limited head-to-head baselines vs human graders (e.g., inter-grader consistency); (iii) under-specified validation (few use stratified k-fold plus an independent test set); (iv) sparse reporting of deployment factors (speed, cost, lighting variation).

Positioning of this study. To address these gaps, this work integrates defect severity, ripeness index, shape uniformity, and size into a unified, non-destructive grading pipeline tailored for Harumanis mangoes [20]. The system is benchmarked against human grading consistency and validated through k-fold cross-validation with an independent test split, reducing overfitting risk and strengthening evidence of real-world applicability.

III. MATERIALS AND METHODS

A. A Structure of Quality Grading System

This study was conducted in multiple orchards across Perlis, where the grading system hardware, shown in Fig. 1, was deployed. To acquire image data and evaluate the geometric parameters of mangoes, the system integrates both image capture and analytical models. The sorting setup consists of two main components. The first is the image processing module, which applies conventional algorithms to transform unstructured image data into structured descriptors and extract external features such as size, color index, shape similarity, and surface defects. Although external features can also be obtained using ML or deep learning methods [23-25], this study employs image processing because of its efficiency, lower computational cost, and ability to operate without extensive training datasets. Moreover, it offers greater flexibility in parameter adjustment compared to ML and deep learning approaches.

The second component combines the extracted features into a comprehensive dataset, which is subsequently used to train ML models. These models classify Harumanis mangoes into four quality categories: PREMIUM, GRADE 1, GRADE 2, and REJECT.

B. Data Preparation for Grading Process

In this study, 1018 samples of mango fruits were used. These mangoes of the Harumanis cultivar were provided by Federal Agricultural Marketing Authority (FAMA) and randomly collected from different commercial orchards located in Perlis. All the fruits without any damage and major defects were selected and classified manually into four ripeness levels by the farmer based on their visual assessment. The farmer manually classified the mangoes into four ripening levels based on peel color. All the data were recorded and classified under the ripeness levels of M1, M2, M3, and M4, respectively. Then, the sample was transported to the lab and inspected by expert workers from FAMA for quality validation.

All the samples were manually measured with respect to their length and width using a mechanical vernier caliper with an accuracy of 0.1 mm. After the data on the geometry dimension was collected, all the samples were weighted using a digital scale with an accuracy of 0.1g to measure the mangoes. To predict the quality of Harumanis mangoes, a data set was made to classify the ripening level, surface defect, shape uniformity, and size that were obtained from selected mangoes. Simultaneously, the classification of quality and grading of the same samples are done by the proposed system using image processing method. This system was configured as shown in Fig. 1.

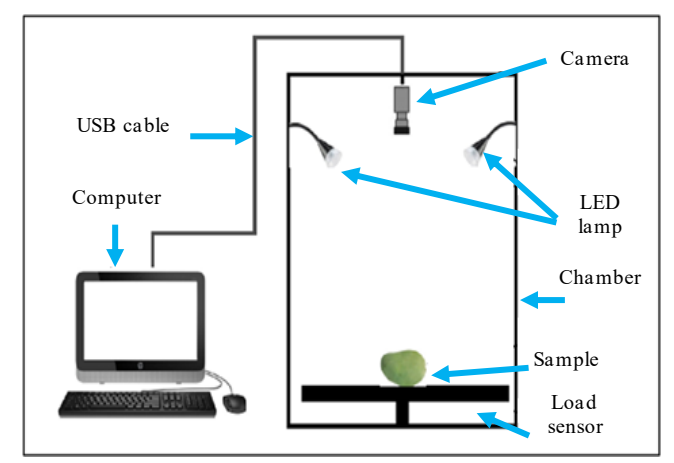


Fig. 1. System configuration for data collection.

The digital camera used for color image acquisition is the Basler acA1600-60gc GigE, with the e2v EV76C570 CMOS sensor that captures images of 1600x1200-pixel resolution. This camera is mounted 400mm on top of the chamber, and the illumination system provides two 10-watt LEDs. A generalized block diagram of the proposed research methodology for quality assessment of Harumanis is shown in Fig. 2.

C. Image Processing

In this work, the research methodology is structured as a sequential pipeline for the quality assessment of Harumanis mangoes, where each stage improves its respective task and provides input to the next. The generalized methodology (Fig. 3) consists of four main parts: 1) image acquisition, 2) image preprocessing and segmentation, 3) feature extraction, and 4) classification.

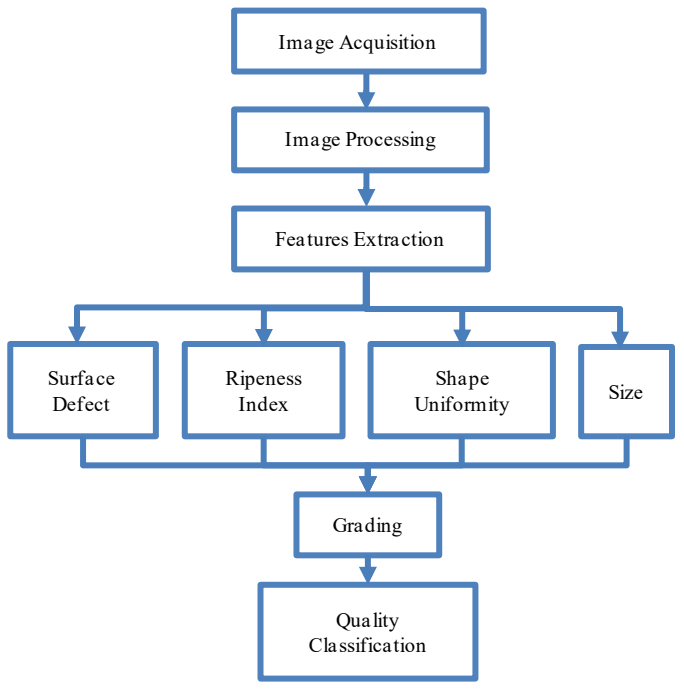


Fig. 2. Block diagram of the image processing technique for quality assessment.



Fig. 3. Block diagram image processing technique.

In the first stage, mango images were captured using a controlled imaging setup with uniform illumination, neutral background, and fixed camera distance to minimize variation. Preprocessing included noise reduction using a Gaussian filter, contrast enhancement with histogram equalization, and background removal through thresholding to isolate the fruit. Segmentation was performed using a combination of color-based thresholding and morphological operations to accurately delineate the mango boundary, as illustrated in Fig. 4.

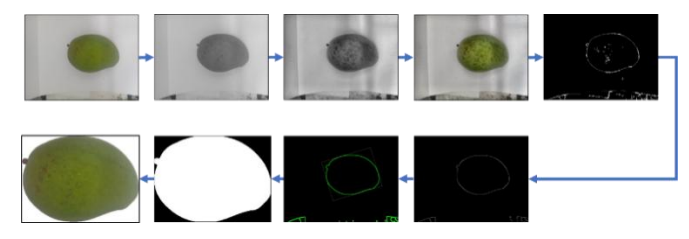


Fig. 4. Image segmentation process.

The second stage, feature extraction, involved computing color features (RGB, HSV, and statistical color moments) and shape descriptors (area, perimeter, eccentricity, Fourier descriptors) from the segmented region. These features were sampled across 1,018 mango images to ensure representativeness of different ripeness stages, sizes, and surface conditions.

Finally, in the classification stage, the extracted features were fed into a Fuzzy Inference System (FIS) to grade ripeness, shape uniformity, and defect severity, while size grading was

conducted by categorizing fruit dimensions into four predefined classes. The configuration of membership functions and rule bases in FIS was optimized through iterative tuning and cross-validation to achieve robust performance.

D. Extracting Mango External Features

The feature extraction stage represents the most critical component of computer vision—based grading, wherein salient numerical descriptors are systematically derived from mango images and extraneous information is eliminated to ensure analytical relevance. In this study, two categories of features were selected—color and shape—because they directly reflect the criteria used in commercial grading of Harumanis mangoes as shown in Fig. 5. Color features were used to capture two important quality aspects: the ripeness index and external defects. Ripeness was quantified by analyzing pixel intensity distributions in RGB and HSV spaces, since skin color transitions from green to yellow or orange are strongly correlated with physiological maturity.

External defects such as bruises, dark spots, and blemishes were detected as localized deviations in color patterns, providing an objective means of assessing defect severity, which is critical for maintaining export quality standards [18], [26]. Shape features, on the other hand, were extracted to evaluate both shape uniformity and fruit size. Geometric descriptors such as aspect ratio, eccentricity, and contour smoothness were applied to determine how well the fruit conforms to the typical elongated-oval profile of Harumanis mangoes, as misshapen fruits are usually downgraded in grading practice.

Size was estimated using dimensional attributes including length, width, and projected area, since fruit size is one of the main determinants of market grade categories such as PREMIUM, GRADE 1, GRADE 2, and REJECT. By integrating these color- and shape-based features, the system provides a robust representation of the visual attributes most relevant to consumer acceptance and commercial value.

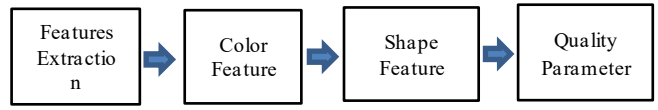


Fig. 5. Block diagram of object detection.

E. Determination of Quality Parameters

1) Surface defects: The evaluation of the Surface Defect Severity Index (SDSI) for fruit entails measuring and quantifying the skin imperfections on fruits. This is a common procedure in the fruit business to assess the quality and marketability of fruits. A numerical scoring system or grading scale is established to assess the severity of problems. This scale ranges from 0 to 5, where 0 indicates no problems, 1 signifies very minor superficial faults, 2 denotes slight superficial defects, 3 represents moderate defects, 4 indicates severe defects, and 5 reflects extremely severe defects, as seen in Table I. To evaluate this score scale, the binary picture is analyzed to determine the quantity of lesions, the cumulative size of the lesions, and the overall area of the mango. The total area of the mango and the area of the defective areas are utilized

to compute the percentage of defect, referred to as PoD. The PoD is often computed using the following equation:

$$PoD = \frac{\text{total area of defected portions}}{\text{area of the entire mango}} * 100 \tag{1}$$

Finally, the value of PoD is used as the input to the FIS to compute the membership functions for the prediction of the Surface Defect Severity Index (SDSI). The measurement of SDSI is based on three methods: PoD_{pc} , which counts pixels to measure area; PoD_{gt} , which uses mathematical analysis to understand spatial relationships; and PoD_{cl} , which divides the area into grid cells for systematic assessment. Additionally, the hybridization method (PoD_{hy}) integrates these approaches to enhance overall accuracy. Together, these methods provide a comprehensive and reliable framework for classifying SDSI.

TABLE I. CLASSIFICATION OF SDSI

Quality Class		Scori ng Scale	% of Defect (PoD)	Inference
Commer	PREMIU M	1≤	0 - 5	Free or very slight superficial defects
cial standard	1	2	5-Oct	Slight superficial defects
	2	3	Oct-15	Moderate defect
Reject	3	4	15 - 40	Severe defect
Reject	4	5	>40	Very severe defect

2) Ripeness index: A fuzzy classifier is used to create the classification system for the ripeness level of the Harumanis mango. The fuzzy logic system has three inputs with a membership function for each input. These three inputs are represented by color measurement of U, Cr and a^* channels that were extracted from the color space of YUV, YCrCb and L^*a^*b , respectively. The determination of the ripeness index is based on the closeness of the values between the ripeness classes in terms of parameters and consumer preferences. Table II presents the mean pixel values for the Cr, U and a^* color channels, which severe as indicators of the ripeness level in Harumanis mangoes. There are 18 rules to be the basis for the input pattern, and the number for the output is four: unripe, underripe, ripe, and overripe. On the other hand, color channels with distinct points of range were employed with triangular membership functions. When values for the color channel are too close together, triangle membership functions have a tendency to overlap.

Concurrently, the output value is being defuzzified using the centroid approach. The set of rules that form the basis of the input pattern that produces an output was displayed by the rule viewer. The membership function combination utilizing the OR operation and the associated output are represented as the rule's viewer. It is composed of four membership functions: unripe, underripe, ripe, and overripe. Since a part of the unripe and overripe membership functions have instantly distinguishable color characteristics, they were trapezoidal in shape. Both the ripe and underripe classifications often have similar values and sometimes even the same color. They were represented by a triangular membership function.

At each level of classification, two types of data are separated into a testing set and a training set in order to validate the model. The value of training data will be a benchmark whose value is used as a differentiator for each class. To determine whether or not the system is operating correctly, test samples are created using the test data from the defuzzification process. Each of the training and test sets of data has 250 of the Harumanis mangos.

TABLE II. HARUMANIS RIPENESS INDEX ESTABLISHED VISUALLY BY THE COLOUR CHANNEL

Ripeness	Co	Scoring		
Index	Cr	U	a*	Scale
M1	≤120	≤116	≤125	1
M2	>120 - 125	>116 - 120	>125 - 130	2
M3	>125 - 130	>120 - 124	>130 - 135	3
M4	>130	>124	>35	4

3) Shape uniformity: The Shape Uniformity Index (SUI) is classified as abnormal if it measures less than 80%, which may be caused by a misshapen, another clone, or grafting with another variety of mangoes. The shape uniformity is based on calculating the degree of uniformity of the sets between the Euclidean distance of the boundaries, and the differences in the parameters of the vertices of areal spatial objects. Fourier descriptors are features that can represent boundary shape of an object. They are scale, translation and rotation invariant. Contour detection was applied to the binary image to identify the largest contour (the mango), and the centroid was obtained from contour image moments. Distance of centroid from contour boundary points were computed and discrete Fourier Transform was calculated. Six standard samples selected by expert are used for comparison. These samples are labeled as T1-T6, with masses ranging from 240 g to 580 g. The Euclidean distance d_E between two vectors is defined using Eq. (2).

$$d_E(G_1, G_2) = \sum_{m=1}^{m=M_p} \sqrt{(|G_1(m)| - |G_2(m)|)^2}$$
 (2)

where, M_p denotes the number of Fourier Descriptors pairs used for matching. G_1 and G_2 is Fourier shape descriptors, and m is the pixels numbered from 0 to m-1 at regularly spaced position. Then, the Euclidean distance, d_E from Eq. (2) is applied to measure the uniformity index of shape. The percentage of uniformity in shape S can be calculated as in the equation below.

$$S = (1 - d_E) * 100 (3)$$

In some cases, the shape of the mango does not look like the original even though it is actually from a Harumanis clone due to the grafting effect. According to Jabatan Pertanian Perlis, they still consider as Well-shaped (WS), although it does not follow the standard shape. Therefore, the half-shape measurement of the uniformity index needs to be performed. This process is repeated with new templates consisting only of half-cut Harumanis shapes for both the lower and upper parts. Then, from Eq. (3), the percentage of uniformity in shape for entire

mango, upper and lower half-cut are calculated and defined S_{Ef} , S_{Eu} and S_{El} , respectively.

To predict SSI, fuzzy classifier is used. The values of these three parameters S_{Ef} , S_{Eu} and S_{El} for are passed as input to fuzzy system and decision has been taken that the mango fruit is HS, WS (well-shaped), and AS (deformed). In designing fuzzy rules for the system, considerations and assumptions obtained from [FAMA] had been taken. The system comprises of eight rules obtained from three inputs and one output of membership functions. Table III shows summary of rules represents by linguistic variable used in system.

TABLE III. IF-THEN RULES FOR CONVERTING FUZZY INPUTS TO FUZZY OUTPUTS

	Input Variabl	Scoring scale (SIII)		
S_{Ef}	S_{Eu}	S_{El}	Scoring scale (SUI)	
>80	>50	>50	1	
>80	>50	<50	1	
>80	<50	>50	1	
>80	<50	<50	2	
<80	>50	>50	2	
<80	<50	>50	3	
<80	>50	<50	3	
<80	<50	<50	4	

4) Size: Optical size grading is a process used in various industries, including agriculture, manufacturing, and quality control, to sort or classify objects based on their size using optical technology [27], [17]. This method involves the use of cameras to capture images of the objects and analyse them into different size categories. Optical size grading is preferred over manual grading in many applications because it offers a fast and efficient way to automate the sorting process, improving productivity and reducing human error. To classify mango size, a fuzzy logic classifier is used. In order to create a modelling system, fuzzy logic allows for the use of size features for variables and imprecise relationships. Two parameters, including weight and area, are employed to determine size features.

TABLE IV. RANGE OF WEIGHT AND AREA PARAMETER FOR SIZE FEATURE

Size	Weight (g)	Area (pixels)	Scoring scale (SI)
Small (S)	<300	<78212	4
Medium (M)	>301-400	>78213 - 101102	3
Large (L)	>401-500	>101103 - 127363	2
Extra Large (XL)	>501	>127364	1

The size feature is initially derived from the range of each individual parameter. These range values will serve as a reference and a range input for the fuzzy classification system. A total of 566 mangoes are used in determining the range value, weight, and area of each category, as shown in Table IV. The

trapezoidal membership function of weight and area is then formed, assigning the proper range to the respective size feature.

F. Machine Learning for Grading Mangoes

The final stage focuses on classifying Harumanis mangoes into quality grades based on various features, following local standards. A dataset of 1018 samples was used to build and validate the classification models. Three supervised ML methods were applied: Multi-Layer Perceptron Neural Networks (MLPNN), Adaptive Neuro-Fuzzy Inference System (ANFIS), and Support Vector Machines (SVM). These methods were chosen for their individual strengths MLPNN handles complex non-linear patterns well [31], ANFIS integrates fuzzy logic for dealing with uncertainty and provides interpretable results [29], while SVM excels in high-dimensional data and resists overfitting with flexible kernel functions [30]. Each method classifies input features into one of several distinct quality classes. Since all dataset parameters are on similar scales, normalization may not be necessary [28].

IV. RESULTS AND DISCUSSION

The study was conducted using a dataset comprising 1,018 Harumanis mango samples. These samples were provided by the Federal Agricultural Marketing Authority and randomly collected from various commercial orchards in Perlis. All fruits selected were free from damage and major defects, and were manually classified into four ripeness indexes by the farmer based on visual assessment. The data was recorded and classified under the ripeness levels of M1, M2, M3, and M4. The results obtained for surface defect estimation, ripeness index, size, shape uniformity index classification, and final grading are discussed in the following sections.

A. Surface Defect Prediction

Fig. 6 shows the comparison of the SDSI index for the actual values (expert-provided) and the predictor methods (PoD_{pc} , PoD_{gt} , PoD_{cl} , and PoD_{hy}) is indicative of distinctions that occur in predictive accuracy across different SDSI categories. In this case SDSI 1, the actual value is around 500, and slightly overestimates PoD_{pc} , as for PoD_{gt} and PoD_{cl} they provide quite equal estimates. PoD_{hy} gives pretty much underestimates value. SDSI 2 reveals a true value much lower (~180) with PoD_{pc} and PoD_{gt} being somehow lower than the real value, whereas PoD_{cl} significantly overestimates it, followed by PoD_{hy} and which is also above the actual value.

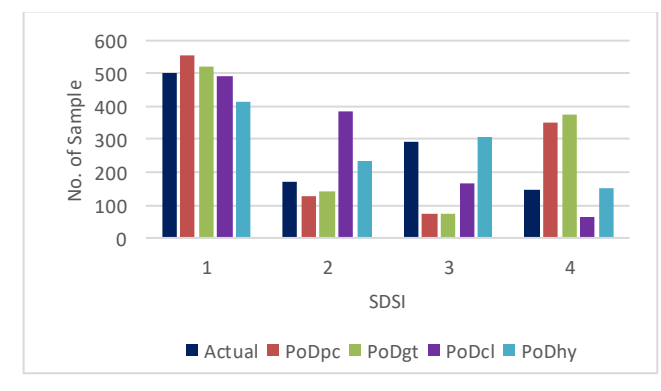


Fig. 6. Comparison of classifying the SDSI.

The actual value and the different predictor methods show SDSI 3, where most methods present lower sums than the actual value (~300), PoD_{pc} and PoD_{qt} being the farthest off. PoD_{hv} gets the nearest value to the actual one that is why it is the most accurate predictor in this category. In the last group named SDSI 4, there is a partial match for PoD_{qt} as the actual value is heavily overestimated by it. For PoD_{pc} the actual value is overestimated as well. PoD_{cl} has underestimated the value massively. PoD_{hy} is slightly overestimated but is closer than the others. In general, PoD_{hy} is found to be a very well-balanced approach that delivers predictions falling inside the correct range of values for various SDSI types. PoD_{pc} and PoD_{qt} mainly vary between the two extremes of under- and overestimation regarding the level of SDSI. PoD_{cl} is not in a steady situation, in SDSI 2 and SDSI 4 especially, it is able to either drastically underestimate or overestimate the issue.

B. Ripeness Index Prediction

From the confusion matrix in Table V, it shows that overall, the ripeness level M1-M4 achieved accuracies above than 90%. M4 groups has only three misclassification and thus attained 95.8% of accuracy. Subsequently, M3, M2 and M1 achieved accuracies with 91.7%, 92.2% and 94.4% accordingly. Seven samples from M3 were misclassified into M4 and M2, respectively. On top of that, 71 out of 77 samples from M2 are correctly classified to their group whilst two sample is misclassified into M3 and four samples in M1. Meanwhile, 51 out 54 image samples from M1 were correctly classified to their group whilst three sample was falsely classified to M2.

TABLE V. CONFUSION MATRIX FOR DETERMINING THE ACCURACY OF FUZZY

Actual	No. of	f Predicted Ripeness Level				Accuracy
Ripeness Level based on Brix	Sample	M1	M2	М3	M4	(%)
M1	54	51	3	0	0	94.4
M2	77	4	71	2	0	92.2
М3	84	0	3	77	4	91.7
M4	72	0	0	3	69	95.8
TOTAL	287			Aver	age	93.5

C. Shape Uniformity Index (SUI) Prediction

The experiment was conducted to evaluate the effectiveness of a proposed method in distinguishing the standard shape of Harumanis mangoes from other categories, specifically well-shaped, and abnormal shape. Each category comprised 1018 samples of mangoes that varied in size. Initially, these samples underwent visual inspection by FAMA staff to assess their shape characteristics, aligning with the conditions for the SUI. The confusion matrix in Table VI showcases a discriminant model utilizing a fuzzy algorithm to predict the quality of Harumanis mangoes based on the SUI, achieving an impressive overall average accuracy of 91.6%.

The model effectively classifies samples across four quality categories: Class 1 (232 samples) with 92.7% accuracy, Class 2 (622 samples) at 87.9%, Class 3 (131 samples) with 88.5%, and Class 4 (368 samples) attaining the highest accuracy of 97.1%. Despite the model's robustness, slight misclassifications

between adjacent quality classes indicate potential for improvement in accurately handling borderline cases. Overall, the results affirm the model's effectiveness in enhancing quality control processes for Harumanis mangoes.

TABLE VI. CONFUSION MATRIX OF DISCRIMINANT MODEL FOR PREDICTING THE QUALITY OF HARUMANIS BASED ON SUI

Subjective	No. of	f Fuzzy algorithm output				Accuracy (%)
classification	Sample	1	2	3	4	
1	250	232	18	0	0	92.8
2	708	56	622	30	0	87.9
3	148	0	10	131	7	88.5
4	379	0	0	11	368	97.1
Average						91.6

D. Size Estimation

The estimated mass, M_{Est} , was further used in classifying Harumanis mangoes into four categories of size classes. Classification results from 1018 Harumanis mangoes samples show the effectiveness of the proposed size prediction using fuzzy logic in categorizing mangoes into four size classes: Small (S), Medium (M), Large (L), and Extra-Large (XL) as shown confusion matrix in Table VII. The confusion matrix reveals that the Harumanis mangoes size prediction model performs well, with most predictions being correct, especially for the XL category. The diagonal elements, which show correct predictions, are dominant, indicating high accuracy. However, some misclassifications occur, particularly between Medium (M) and Large (L) sizes, where Medium (M) mangoes are sometimes mistaken for Large (L) ones (0.99%). There are also a few cases where Large (L) mangoes are predicted as Extra-Large (XL) with 2.01%. Although there are some misclassifications, the overall accuracy is still strong. These errors are relatively small compared to the correct predictions, but they suggest that the model could benefit from further refinement, especially in distinguishing between Medium (M) and Large (L) sizes.

TABLE VII. CONFUSION MATRIX FOR SIZE PREDICTION

Actual	Size		Accuracy			
Category	Total	S M L XL				(%)
S	196	191	5	0	0	97.5
M	505	8	492	5	0	97.4
L	547	0	10	526	11	96.3
XL	210	0	0	3	207	98.6

TABLE VIII. CLASSIFICATION RESULTS OF COMPLETE SAMPLES INTO SIZE

A - 41 C'	Prediction Performance (%)					
Actual Size	Precision	Recall	F1-Score			
S	97.76	97.32	97.54			
M	96.3	97.41	96.85			
L	97.2	96.19	96.7			
XL	98.93	98.23	98.39			

Table VIII shows the analysis of the mango size prediction model demonstrates strong performance across all size categories. The model exhibits high Precision, with Extra-Large (XL) mangoes having the highest value at 98.6%, indicating that when the model predicts Extra-Large (XL), it is almost always correct. Small (S) and Large (L) categories also show very high Precision scores of 97.76% and 97.20%, respectively, while Medium (M) has a slightly lower Precision at 96.30%.

In terms of Recall, which measures how well the model identifies all instances of each size, XL mangoes again perform the best with a Recall of 98.23%, ensuring that few XL mangoes are missed. The Small (S) category follows closely with a Recall of 97.42%. However, Large (L) has a slightly lower Recall of 96.19%, likely due to some misclassifications with Medium (M) mangoes. The F1-Score, which balances both Precision and Recall, also shows that the model performs well overall, with Extra-Large (XL) leading at 98.93%, followed by Small (S) at

97.54%. While Medium (M) and Large (L) have slightly lower F1-Scores of 96.85% and 96.70%, respectively, they still reflect strong performance.

E. Quality Classification

Table IX summarizes the evaluation of multiple classification models. The performance of seven different models, including ANFIS, MLPNN, SVM, SVM+ PoD_{pc} , SVM+ PoD_{gt} , SVM+ PoD_{cl} , and SVM+ PoD_{hy} , was analyzed based on various evaluation metrics such as Mean Absolute Error (MAE), Mean Squared Error (MSE), Root Mean Squared Error (RMSE), Accuracy, Precision, Recall, and F1-Score. The results indicate significant differences in how well each model handles classification tasks.

TABLE IX. PERFORMANCE COMPARISON ACROSS PREDICTORS

Predictor	MAE	MSE	RMSE	Accuracy (%)	Precision	Recall	F1-Score
ANFIS	120.3	150.5	12.3	81.6	0.78	0.81	0.79
MLPNN	90.2	110.4	10.5	86.8	0.83	0.86	0.84
SVM	85.5	102.2	10.1	87.5	0.85	0.88	0.86
$SVM+PoD_{pc}$	98.6	115.3	10.7	83	0.81	0.83	0.82
\mathbf{SVM} + PoD_{gt}	95.2	113.7	10.6	83.6	0.82	0.85	0.83
SVM+PoD _{cl}	180.4	210.6	14.5	65.5	0.65	0.67	0.66
SVM+PoD _{hy}	70.3	95.2	9.8	95.1	0.91	0.94	0.92

Among the base models, SVM demonstrated the highest accuracy (87.5%), outperforming both MLPNN (86.8%) and ANFIS (81.6%). SVM also had the lowest error rates, with an MAE of 85.5 and RMSE of 10.1, meaning it made fewer misclassifications compared to the other standalone models. While MLPNN performed better than ANFIS, it still had a slightly higher error rate than SVM, making SVM the best base model overall.

When additional enhancements were applied, SVM+ PoD_{hy} emerged as the best model overall, achieving the highest accuracy of 95.1% and the lowest MAE (70.3) and RMSE (9.8), indicating that it had the fewest misclassifications and highest precision. Furthermore, its recall of 0.94 and F1-score of 0.92 confirm that SVM+ PoD_{hy} had the best balance between correctly identifying positives while minimizing false positives and false negatives.

This makes SVM+ PoD_{hy} the most reliable predictor among all models tested. On the other hand, SVM+ PoD_{cl} performed the worst, with an accuracy of only 65.5% and a significantly higher error rate (MAE of 180.4 and RMSE of 14.5). This indicates that adding the clustering-based PoD_{cl} method to SVM led to higher misclassifications, making it the least effective enhancement.

The models SVM+ PoD_{pc} (83.0%) and SVM+ PoD_{gt} (83.6%) showed moderate improvements but did not surpass the accuracy of SVM alone (87.5%), meaning that these modifications did not significantly improve performance. Their error rates were slightly lower than ANFIS but remained higher than standard SVM, suggesting that PoD_{pc} and PoD_{gt} did not contribute substantially to classification accuracy.

Overall, SVM+ PoD_{hy} was the most successful model, achieving the highest accuracy, lowest error rates, and best balance between precision and recall. In contrast, SVM+ PoD_{cl} was the weakest model, suffering from high misclassification rates and poor overall performance. The findings suggest that SVM alone is a strong predictor, but hybrid methods like PoD_{hy} significantly enhance its capabilities, while others, such as PoD_{cl} , may introduce inefficiencies.

V. Conclusion

This study demonstrates a robust image-based framework for non-destructive quality assessment of Harumanis mangoes by integrating surface defect severity, ripeness index, shape uniformity, and size into a unified grading system. Using fuzzy inference and ML models, with SVM+ achieving the highest accuracy of 95.1%, the system clearly outperformed traditional manual grading. While the approach shows strong potential, limitations include reliance on a single cultivar and controlled imaging conditions, which may restrict generalizability. Future work will extend validation to multiple cultivars under realworld conditions, explore deep learning for richer feature extraction, and investigate real-time deployment to support scalable adoption in post-harvest supply chains.

ACKNOWLEDGMENT

The authors gratefully acknowledge the technical staff and agricultural experts from the Institute of Sustainable Agrotechnology, Universiti Malaysia Perlis, for their valuable support and contributions.

REFERENCES

- [1] N. Nasron, N. S. Ghazali, N. M. Shahidin, A. A. Mohamad, S. A. Pugi, and N. M. Razi, "Soil suitability Assessment for Harumanis Mango Cultivation in UITM Arau, Perlis," IOP Conference Series Earth and Environmental Science, vol. 620, no. 1, p. 012007, Jan. 2021, doi: 10.1088/1755-1315/620/1/012007.
- [2] R. Ningtyas, P. Gunawan, M. Muryeti, and S. Imam, "APPLICATION OF INTELLIGENT LABEL IN MONITORING THE PHYSICAL AND CHEMICAL QUALITY OF MANGO MANALIGA (MANGIFERA INDICAL)," Andalasian International Journal of Agriculture and Natural Sciences (AIJANS), vol. 3, no. 01, pp. 37–46, Mar. 2022, doi: 10.25077/aijans.v3.i01.37-46.2022.
- [3] M. L. Ntsoane, M. Zude-Sasse, P. Mahajan, and D. Sivakumar, "Quality assessment and postharvest technology of mango: A review of its current status and future perspectives," Scientia Horticulturae, vol. 249, pp. 77–85, Jan. 2019, doi: 10.1016/j.scienta.2019.01.033.
- [4] N. T. M. Long and N. T. Thinh, "Using machine learning to grade the Mango's quality based on external features captured by Vision System," Applied Sciences, vol. 10, no. 17, p. 5775, Aug. 2020, doi: 10.3390/app10175775.
- [5] T. Mon and N. ZarAung, "Vision based volume estimation method for automatic mango grading system," Biosystems Engineering, vol. 198, pp. 338–349, Sep. 2020, doi: 10.1016/j.biosystemseng.2020.08.021.
- [6] K. A. B. Ahmad, M. Othman, S. L. S. Abdullah, N. R. Ali, and S. R. M. Dawam, "Mango shape maturity classification using image processing," International Conference and Workshops on Recent Advances and Innovations in Engineering (ICRAIE), pp. 1-5, Nov. 2019, doi: 10.1109/icraie47735.2019.9037776.
- [7] M. H. B. Ismail, T. R. Razak, R. A. J. M. Gining, and S. S. M. Fauzi, "Simulating Bruise and Defects on Mango images using Image-to-Image Translation Generative Adversarial Networks," International Conference on Artificial Intelligence and Data Sciences (AiDAS, pp. 110–114, Sep. 2022, doi: 10.1109/aidas56890.2022.9918816.
- [8] C. Yao et al., "Detection storage time of mangoes after mild bruise based on hyperspectral imaging combined with deep learning," Journal of Chemometrics, vol. 38, no. 9, May 2024, doi: 10.1002/cem.3559.
- [9] R. Nithya, B. Santhi, R. Manikandan, M. Rahimi, and A. H. Gandomi, "Computer Vision system for mango fruit defect detection using deep convolutional neural network," Foods, vol. 11, no. 21, p. 3483, Nov. 2022, doi: 10.3390/foods11213483.
- [10] Naik, S., & Patel, B. (2017). Thermal imaging with fuzzy classifier for maturity and size based non-destructive mango (Mangifera Indica L.) grading. In International Conference on Emerging Trends & Innovation in ICT (ICEI). https://doi.org/10.1109/etiict.2017.7977003
- [11] D. Worasawate, P. Sakunasinha, and S. Chiangga, "Automatic classification of the ripeness stage of mango fruit using a machine learning approach," AgriEngineering, vol. 4, no. 1, pp. 32–47, Jan. 2022, doi: 10.3390/agriengineering4010003.
- [12] F. S. Mim, S. Md. Galib, Md. F. Hasan, and S. A. Jerin, "Automatic detection of mango ripening stages – An application of information technology to botany," Scientia Horticulturae, vol. 237, pp. 156–163, Apr. 2018, doi: 10.1016/j.scienta.2018.03.057.
- [13] J. Aguirre-Radilla, E. De La Cruz-Gámez, J. L. Hernández-Hernández, J. Carranza-Gómez, J. A. Montero-Valverde, and M. Martínez-Arroyo, "Texture and Color-Based Analysis to determine the quality of the Manila mango using digital image processing techniques," in Communications in computer and information science, 2022, pp. 93–106. doi: 10.1007/978-3-031-19961-5_7.
- [14] M. A. Momin, M. T. Rahman, Sultana, C. Igathinathane, A. T. M. Ziauddin, and T. E. Grift, "Geometry-based mass grading of mango fruits using image processing," Information Processing in Agriculture, vol. 4, no. 2, pp. 150–160, Apr. 2017, doi: 10.1016/j.inpa.2017.03.003.
- [15] N. Gururaj, V. Vinod, and K. Vijayakumar, "Deep grading of mangoes using Convolutional Neural Network and Computer Vision," Multimedia

- Tools and Applications, vol. 82, no. 25, pp. 39525–39550, Jul. 2022, doi: 10.1007/s11042-021-11616-2.
- [16] A. D. Supekar and M. Wakode. "Multi-Parameter Based Mango Grading Using Image Processing and Machine Learning Techniques". INFOCOMP. vol. 19. no. 2. Dec. 2020.
- [17] W. Aung, T. T. Thu, H. T. D. Aye, P. P. Htun and N. Aung. "Weight Estimation of Mango from Single Visible Fruit Surface using Computer Vision". Sep. 2020. 10.23919/sice48898.2020.9240422.
- [18] J. D. R. Cid, W. Perez-Bailon, L. Rosas-Arias, D. R. Ocampo and J. A. Lopez-Tello. "Design of a Size Sorting Machine Based on Machine Vision for Mexican Exportation Mangoes". Nov. 2018. 10.1109/ropec.2018.8661378.
- [19] K. Utai, M. Nagle, S. Hämmerle, W. Spreer, B. Mahayothee and J. Müller. "Mass estimation of mango fruits (Mangifera indica L., cv. 'Nam Dokmai') by linking image processing and artificial neural network". Elsevier BV. vol. 12. no. 1. pp. 103-110. Jan. 2019. 10.1016/j.eaef.2018.10.003.
- [20] O. P. Zhen, N. Hashim and B. Maringgal. "Quality evaluation of mango using non-destructive approaches: A review". vol. 1. no. 1. pp. 1-8. Mar. 2020. 10.37865/jafe.2020.0003.
- [21] B. Zheng and T. Huang. "Mango Grading System Based on Optimized Convolutional Neural Network". Hindawi Publishing Corporation. vol. 2021. pp. 1-11. Sep. 2021. 10.1155/2021/2652487.
- [22] S. J. Olakanmi, D. S. Jayas and J. Paliwal. "Applications of imaging systems for the assessment of quality characteristics of bread and other baked goods: A review". Wiley. vol. 22. no. 3. pp. 1817-1838. Mar. 2023. 10.1111/1541-4337.13131.
- [23] S. M. T. Islam, S. M. T. Islam, Md. Nurullah, M. Nurullah, Md. Samsuzzaman, and M. Samsuzzaman, "Mango Fruit's Maturity Status Specification Based on Machine Learning using Image Processing," 2017 IEEE Region 10 Symposium (TENSYMP), pp. 1355–1358, Jan. 2020, doi: 10.1109/tensymp50017.2020.9230951.
- [24] L. Chen, T. He, Z. Li, W. Zheng, S. An and L. Zhangzhong. "Grading method for tomato multi-view shape using machine vision". Chinese Society of Agricultural Engineering. vol. 16. no. 6. pp. 184-196. Jan. 2023.10.25165/j.ijabe.20231606.7768.
- [25] M. J. Feldmann et al., "Multi-dimensional machine learning approaches for fruit shape phenotyping in strawberry," Giga Science, vol. 9, no. 5, Apr. 2020, doi: 10.1093/gigascience/giaa030.
- [26] N. Puspitasari, A. M. Kiloes, and J. A. Syah, "Factors affecting sustainability of increasing mango export: an application of MICMAC method," IOP Conference Series Earth and Environmental Science, vol. 892, no. 1, p. 012101, Nov. 2021, doi: 10.1088/1755-1315/892/1/012101.
- [27] N. M. Trieu and N. T. Thinh, "Quality classification of dragon fruits based on external performance using a convolutional neural network," Applied Sciences, vol. 11, no. 22, p. 10558, Nov. 2021, doi: 10.3390/app112210558.
- [28] D. Singh and B. Singh, "Investigating the impact of data normalization on classification performance," Applied Soft Computing, vol. 97, p. 105524, May 2019, doi: 10.1016/j.asoc.2019.105524.
- [29] S. Seoni, V. Jahmunah, M. Salvi, P. D. Barua, F. Molinari, and U. R. Acharya, "Application of uncertainty quantification to artificial intelligence in healthcare: A review of last decade (2013–2023)," Computers in Biology and Medicine, vol. 165, p. 107441, Sep. 2023, doi: 10.1016/j.compbiomed.2023.107441.
- [30] B. Ghaddar and J. Naoum-Sawaya, "High dimensional data classification and feature selection using support vector machines," European Journal of Operational Research, vol. 265, no. 3, pp. 993–1004, Sep. 2017, doi: 10.1016/j.ejor.2017.08.040.
- [31] H. Jin, Y.-G. Kim, Z. Jin, A. A. Rushchite, and A. S. Al-Shati, "Optimization and analysis of bioenergy production using machine learning modeling: Multi-layer perceptron, Gaussian processes regression, K-nearest neighbors, and Artificial neural network models," Energy Reports, vol. 8, pp. 13979–13996, Oct. 2022, doi: 10.1016/j.egyr.2022.10.334.